## PROCEEDINGS OF SPIE

SPIEDigitalLibrary.org/conference-proceedings-of-spie

# Polarization enhancement of passive SWIR cloud thermodynamic phase remote sensing

Martin Jan Tauc, Elizabeth M. Rehbein, Laura M. Eshelman, Joseph A. Shaw

Martin Jan Tauc, Elizabeth M. Rehbein, Laura M. Eshelman, Joseph A. Shaw, "Polarization enhancement of passive SWIR cloud thermodynamic phase remote sensing," Proc. SPIE 11132, Polarization Science and Remote Sensing IX, 1113206 (6 September 2019); doi: 10.1117/12.2530128



Event: SPIE Optical Engineering + Applications, 2019, San Diego, California, United States

## Polarization enhancement of passive SWIR cloud thermodynamic phase remote sensing

Martin Jan Tauc<sup>a</sup>, Elizabeth M. Rehbein<sup>a</sup>, Laura M. Eshelman<sup>a,b</sup>, and Joseph A. Shaw<sup>a,\*</sup>

<sup>a</sup>Department of Electrical and Computer Engineering, Montana State University, 610 Cobleigh Hall, Bozeman, Montana 59717, USA

<sup>b</sup>Currently at Polaris Sensor Technologies Inc., 200 West Side Square, Suite 320, Huntsville, Alabama 35801, USA

#### ABSTRACT

Determining whether a cloud is composed of spherical water droplets of polyhedral ice crystals (i.e., the thermodynamic phase) from a passive remote sensing instrument is very difficult because of the immense variety of clouds and their highly variable microphysical properties. To improve upon the popular method of radiance ratios, we enhance the classification ability by adding polarimetric sensitivity to an instrument that measures radiance in three short-wave infrared bands. Clouds typically induce a polarization signature on the order of a percent, and so sensitive optics are required for accurate classification. In this paper, we present the combination of spectral and polarimetric sensitivity for cloud thermodynamic phase classification using data from a ground-based, 3-band, short-wave infrared polarimeter and cloud-phase validation from a dual-polarization lidar. We then analyze the classification quality of various methods using surface-fitting techniques to show that the addition of polarimetry is advantageous for cloud classification.

**Keywords:** Remote sensing, polarimetry, atmospheric science

#### 1. INTRODUCTION

Clouds are one of the most important factors in weather and climate, but they also carry a large amount of uncertainty, <sup>1-3</sup> thus plaguing the current understanding of global and local climates. The details of how clouds influence climates are very complex, <sup>4-8</sup> and far out of the scope of this paper, but in general the thermodynamic phase of a cloud (i.e., whether it is composed of liquid-water droplets, polyhedral ice crystals, or both) requires further study for two main reasons. First, the cloud thermodynamic phase (CTP) in and of itself can impact how solar radiation either warms or cools the Earth; and second, the CTP must be known prior to identifying other cloud microphysical properties.<sup>3,9-14</sup> For this reason, this paper explores remote sensing techniques for CTP retrieval, specifically by adding polarization sensitivity to the well-established method of radiance ratios.

Recently, we published a conference proceeding paper describing the development of an approach using three radiance ratios constructed from bands centered at  $1.55\,\mu\text{m}$ ,  $1.64\,\mu\text{m}$ , and  $1.70\,\mu\text{m}$  and presented some preliminary data.<sup>15</sup> The data were analyzed using either 3 radiance ratios or the  $S_1$  Stokes parameter separately. Independently, the two methods were able to determine CTP for liquid-water and ice clouds, but only for a very limited data set (the radiance ratio method generally works well for large cloud optical depth and the polarization method generally works well for low cloud optical depth). That paper did not account for more general circumstances when cloud conditions become more complex, and thus did not need to combine the methods to determine CTP under a greater variety of conditions.

In this paper, we use an updated version of the same instrument that has been rebuilt and recalibrated, and therefore we analyze a completely new data set. This data set has a much broader variety of clouds since it was collected on 24 different days during the first six months of 2019. We define the radiance ratios in the same way,

Further author information: (Send correspondence to Joseph A. Shaw) Joseph A. Shaw: E-mail: joseph.shaw@montana.edu, Telephone: (406) 994-7261

Polarization Science and Remote Sensing IX, edited by Julia M. Craven, Joseph A. Shaw, Frans Snik, Proc. of SPIE Vol. 11132, 1113206 · © 2019 SPIE · CCC code: 0277-786X/19/\$21 · doi: 10.1117/12.2530128

$$R_{1.70,1.64} = \frac{L_{1.70} - L_{1.64}}{L_{1.64}},\tag{1}$$

$$R_{1.55,1.64} = \frac{L_{1.55} - L_{1.64}}{L_{1.64}}$$
, and (2)

$$R_{1.55,1.70} = \frac{L_{1.55} - L_{1.70}}{L_{1.70}},\tag{3}$$

and we defined the  $S_1$  Stokes parameter as

$$S_1 = L_{\parallel} - L_{\perp},\tag{4}$$

where  $L_{\parallel}$  and  $L_{\perp}$  are the radiance detected in the planes parallel and perpendicular to the scattering plane, respectively.

#### 2. METHODS

The new version of the SWIR 3-channel polarimeter had the same optical elements as before, but with updates that included new temperature monitoring and control circuitry; a photograph of the inside of the instrument is given in Figure 1. The greatest differences were in the calibrations. The polarimeter underwent more thorough radiometric and polarimetric calibrations and was spectrally calibrated for the first time.

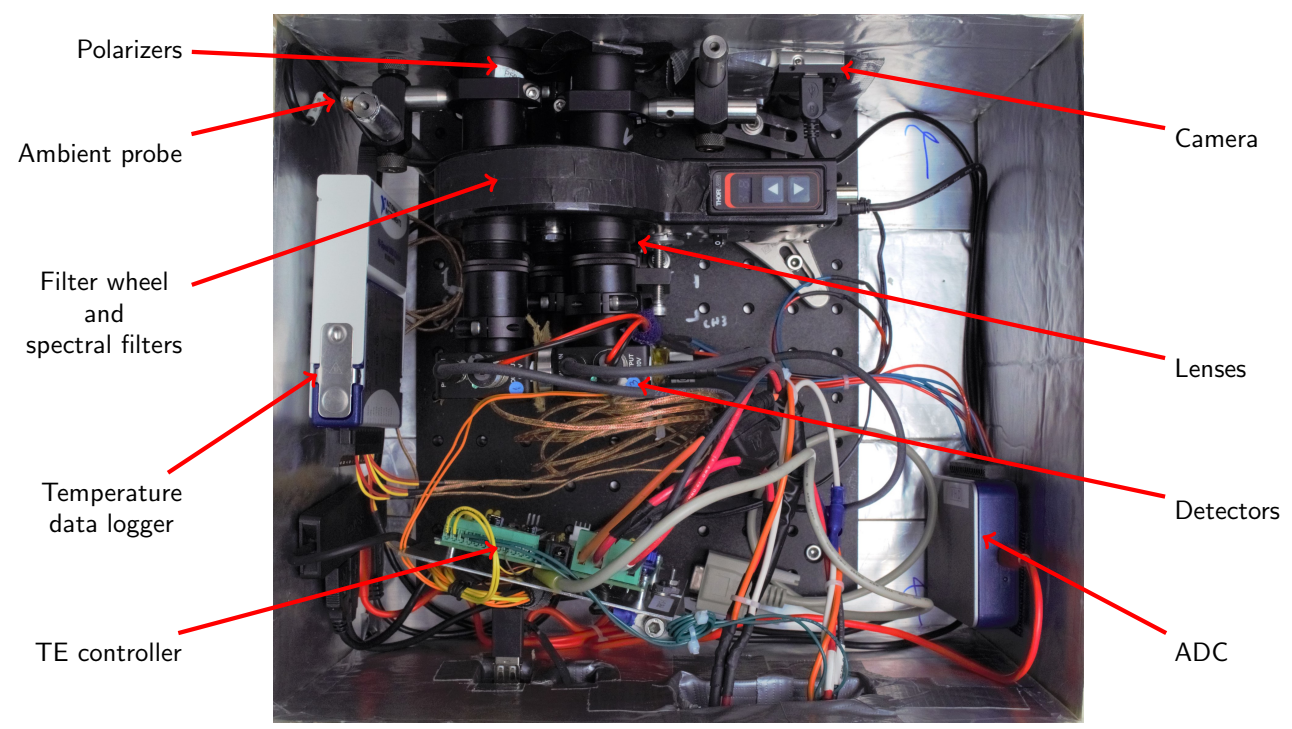


Figure 1. A photograph of the internal components of the SWIR 3-channel polarimeter shows the optical components and the electronics.

#### 2.1 Calibrations

In previous work, only the theoretical (or typical) spectral response of each channel was considered. Outside of a good understanding of the spectral response, this mainly influenced the radiometric calibration. For an experimental calibration, a monochromator swept from 1.45 µm to 1.80 µm for every spectral filter and polarizer combination for a total of 9 spectral calibrations. The normalized spectral responses are shown in Figure 2, where the dashed lines represent the theoretical spectral responses. The experimental and theoretical values are close, but have noticeable differences.

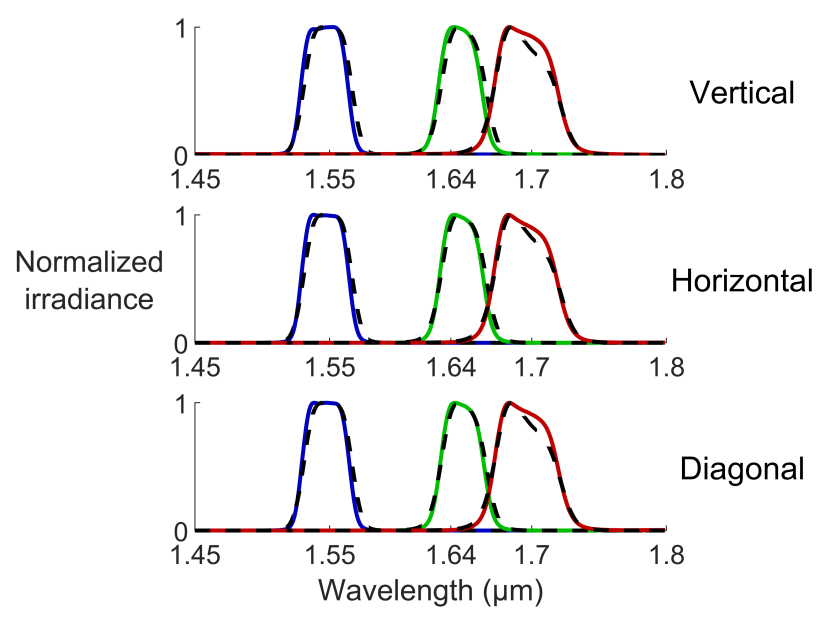


Figure 2. The normalized passbands for every combination of spectral and polarimetric channel were similar in bandwidth to each other and to the theoretical passband (black dashed line).

The field of view calibration showed that the horizontal (or perpedicular) and vertical (or parallel) channels were fairly well aligned, whereas the diagonal channel (at  $45^{\circ}$ ) was only partly aligned with the other two. The diagonal channel was not used in the primary analysis, so the misalignment was not an issue. The fields of view are represented in Figure 3, and each channel had a full-angle field of view of approximately  $2.6^{\circ}$ .

The radiometric and polarimetric calibrations were also done for all 9 spectral and polarization combinations. Their details, along with the field of view calibration, can be found in a dissertation, <sup>16</sup> but overall, the relationship between detected radiance and detector signal was weakly quadratic, and each polarizer was within a degree of its relative orientation. During the polarimetric calibration, double reflections from wire-grid polarizers were quantified and these details are published.<sup>17</sup>

#### 2.2 Experiments

Data were collected over the course of many days starting in January of 2019. The SWIR 3-channel polarimeter was mounted to a pan-and-tilt mount on the roof of a six-story building next to a dual-polarization lidar system, as shown in Figure 4. The polarimeter would orient into the scattering plane defined by the sun, scattering medium (which was always at the zenith), and the instrument. At the same time, the dual-polarization lidar system, an established method of CTP retrieval, 9, 13, 18-22 would operate to determine the CTP. The data from the SWIR 3-channel polarimeter were coded as liquid water or ice depending on the dual-polarization lidar. Data collection took place during cloudy conditions at a variety of solar elevation angles. Clouds varied in cloud optical depth and thermodynamic phase. The data in this paper only consider cases where the CTP was exclusively liquid water or ice. Although mixed phase and mixed layer clouds are common and important, classifying such clouds is out of the scope of this work.

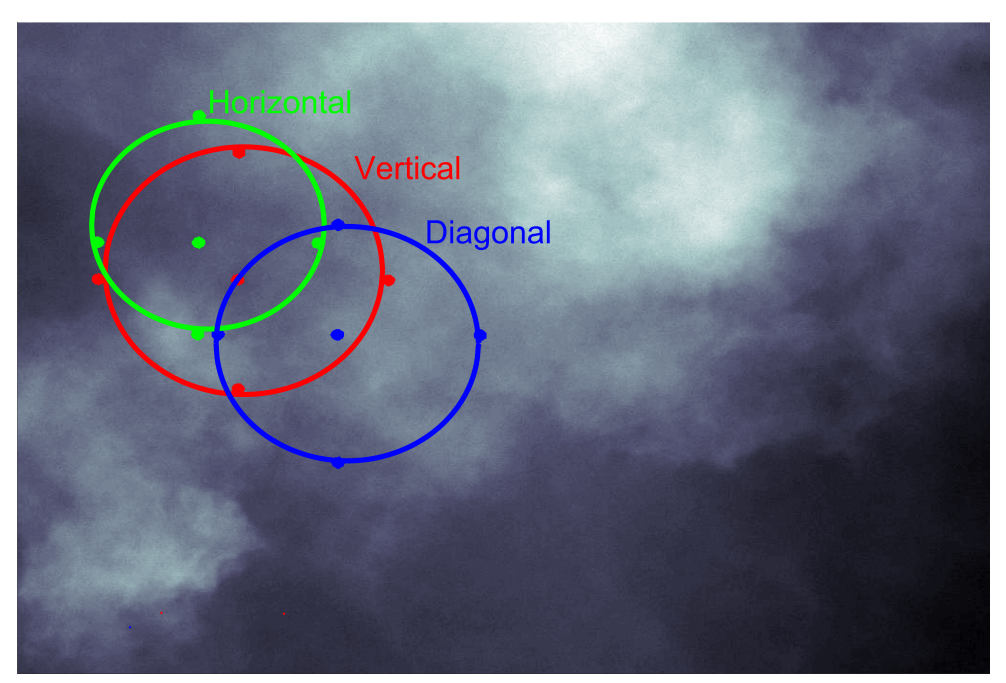


Figure 3. A representation of the FOV for each of the three channels of the polarimeter mapped onto an example image. The vertical and horizontal FOVs are slightly different, but mostly overlap, whereas the diagonal channel has poor overlap with the other two.

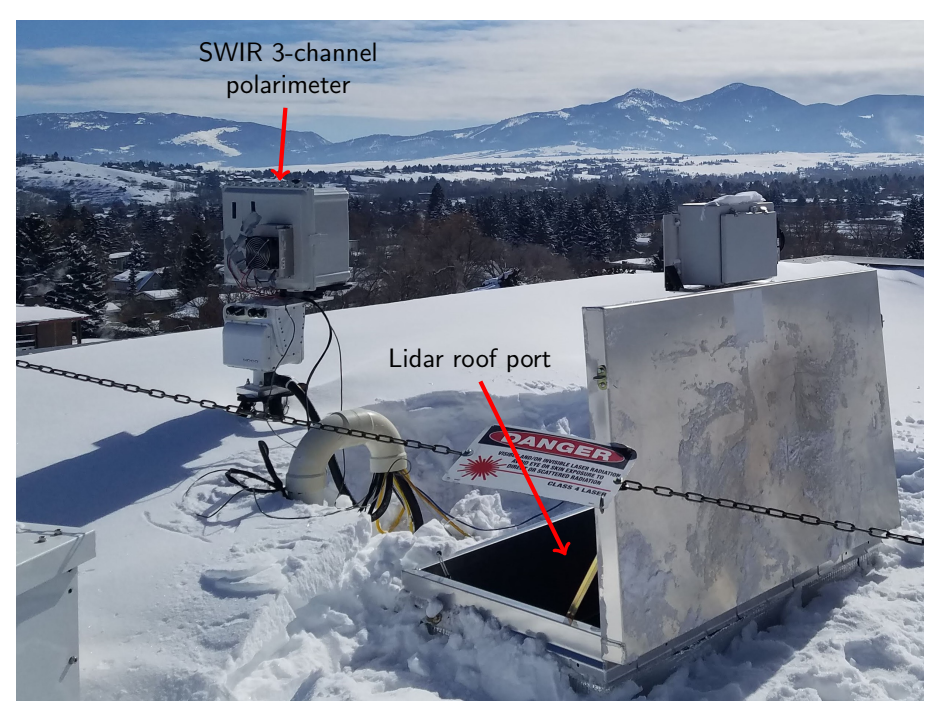


Figure 4. A photograph of the SWIR 3-channel polarimeter and the dual-polarization lidar during a typical experiment. The polarimeter was about 1 m from the laser beam and so the two instruments were looking near the same part of the sky.

After data were collected, the dual-polarization lidar data were analyzed to find cases of isolated liquid water clouds or isolated ice clouds. Then, SWIR 3-channel polarimeter data that temporally aligned with the dual-polarization lidar were flagged for further analysis. Due to a bad cable within the instrument, approximately 55 % of data were contaminated with anomalously high noise and discarded. The final SWIR 3-channel polarimeter data were analyzed to determine if polarimetry improved the separation between liquid-water and ice clouds.

#### 3. RESULTS

In our previous conference proceeding,<sup>15</sup> data were either analyzed with the radiance ratio method or with the polarimetric method, but the data were not examined with a combined method. In this paper, we describe a new classification method, called the combined method, which simultaneously uses radiance ratios and polarimetry to identify CTP.

The radiance ratio method of classifying CTP (which we used as the "control" or "standard" method) showed good separation between liquid-water and ice clouds. Figure 5 shows the liquid-water clouds (as blue circles) and ice clouds (as red triangles); the ice data dominate the upper left hand portion of the figure and are clustered tightly, whereas the liquid-water data dominate the lower portion of the figure and are quite spread out. Nonetheless, the two phases are easy to distinguish except for the region toward the lower right, where ice clouds begin to enter the region dominated by liquid-water clouds. This region represents instances with low cloud optical depth and the where the radiance ratio method breaks down. <sup>15,16</sup>

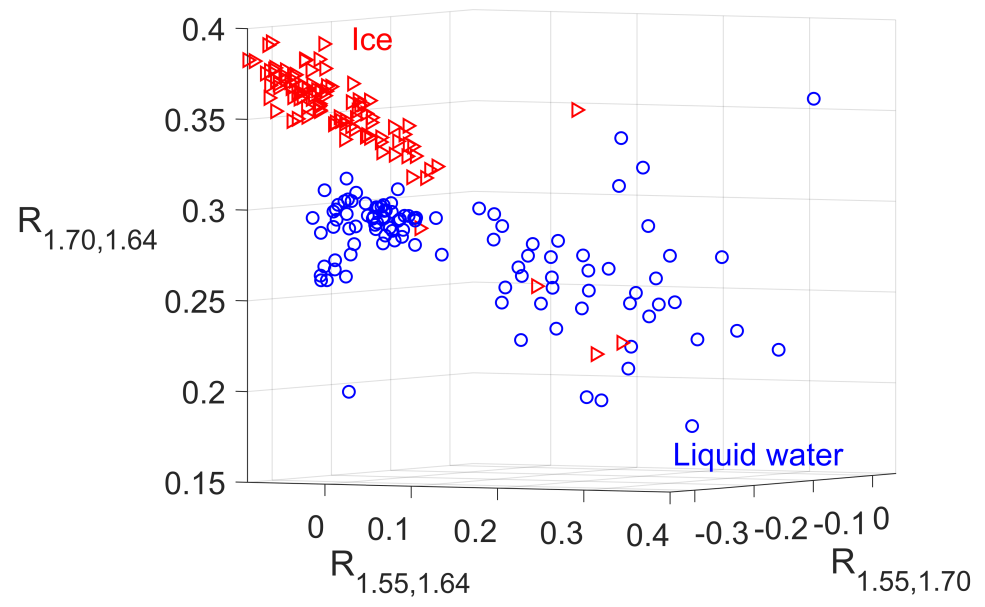


Figure 5. The radiance ratio method separated liquid-water and ice clouds well and CTP began to mix when cloud optical depth was low.

The polarimetric method uses the  $S_1$  Stokes parameter for CTP retrieval and has a strong dependence on scattering angle. Figure 6 plots the  $S_1$  parameter as a function of scattering angle in each of the three spectral bands. It shows that, on average, the ice data were more negative than liquid-water clouds. According to the theory,<sup>23</sup> ice clouds should be negative at scattering angles above 35°, which is the case, but liquid water clouds were expected to be positive. Even so, liquid-water clouds trended toward positive values and showed decent separation from ice clouds despite some mixing between the two phases.

As a means to quantitatively determine whether polarization improves classification ability, we used a method of plane fitting in 3-parameter space, where one plane was fit to the liquid-water data and a separate plane was fit to the ice data, and classification quality was assessed by counting the number of instances where a datum

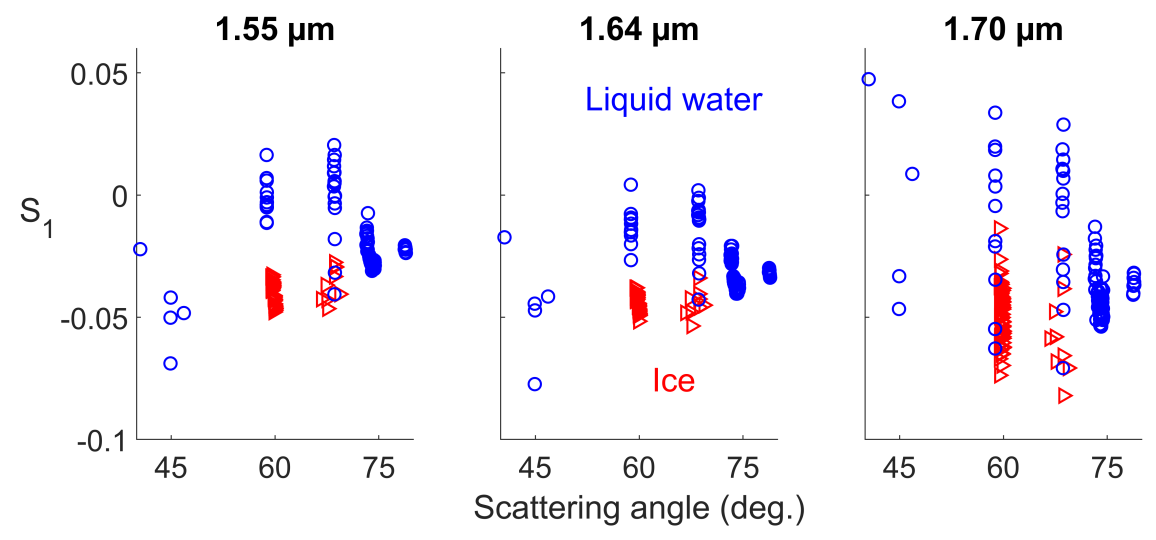


Figure 6. The  $S_1$  Stokes parameter showed decent separation between liquid-water and ice clouds.

was closer to its corresponding-phase phase (more details are give in a dissertation  $^{16}$ ). Nine different parameters were permutated on the 3-parameter space for a total of 84 combinations. The parameters were the three radiance ratios (as shown in Figure 5), the three  $S_1$  parameters (one for each spectral band), and three  $S_0$  parameters (again, one for each spectral band). By changing the parameter space and then assessing the quality of classification, we found that the best 3-parameter space included at least one  $S_1$  parameter; in other words, polarization helped with CTP classification.

Specifically, the combined method consisted of the 3-parameter space of  $R_{1.55,1.64}$ ,  $S_{1,1.64}$  (the  $S_1$  parameter in the 1.64-µm band), and  $S_{0,1.64}$  (the  $S_0$  parameter in the 1.64-µm band). In this 3-parameter space, plotted in Figure 7, the algorithm correctly classified 97.5% of clouds whereas, at best, the radiance ratio method correctly classified only 93.1% of clouds. Although the differences between the two classification values is not huge, it shows that the addition of polarization improves classification. Furthermore, these conditions may have already been favorable to the radiance ratio method (i.e., clouds with large optical depths), and so the addition of polarimetry was minimal.

The polarimeter also suffered from temporal polarimetric artifacts. The total acquisition time of the division-of-time polarimeter was about ten seconds, and in that time clouds could move significantly, thus causing polarimetric artifacts when calculating  $S_1$ . Moving toward a division-of-focal-plane snapshot polarimeter would reduce some of the major drawbacks of the SWIR 3-channel polarimeter.

#### 4. CONCLUSION

This paper builds on the instrument and work presented in Tauc et al.<sup>15</sup> By updating and recalibrating the SWIR 3-channel polarimeter, we got a more robust data set that eventually showed that the addition of polarization was helpful. Previously, the radiance ratio method and polarimetric method had only been compared independently. In this paper, however, the merging of the two theories into the combined method provided the best separation between liquid-water and ice clouds.

The limited data set did not provide a full validation of the strengths and weaknesses of the combined method, but it was the first step in experimentally validating the theory that the combined method is superior to either method independently. Furthermore, when we relaxed some of the conditions used when pre-processing the data, we found that the separation between the two CTPs does become worse, but some form of the combined method (which includes both polarization and radiance) always produced the best classification, further suggesting that polarization helps with CTP discrimination.

In the long term, an instrument such as the SWIR 3-channel polarimeter could be refined into more robust and sensitive instruments that could be spread across the world in a network, much like the AERONET<sup>24</sup>

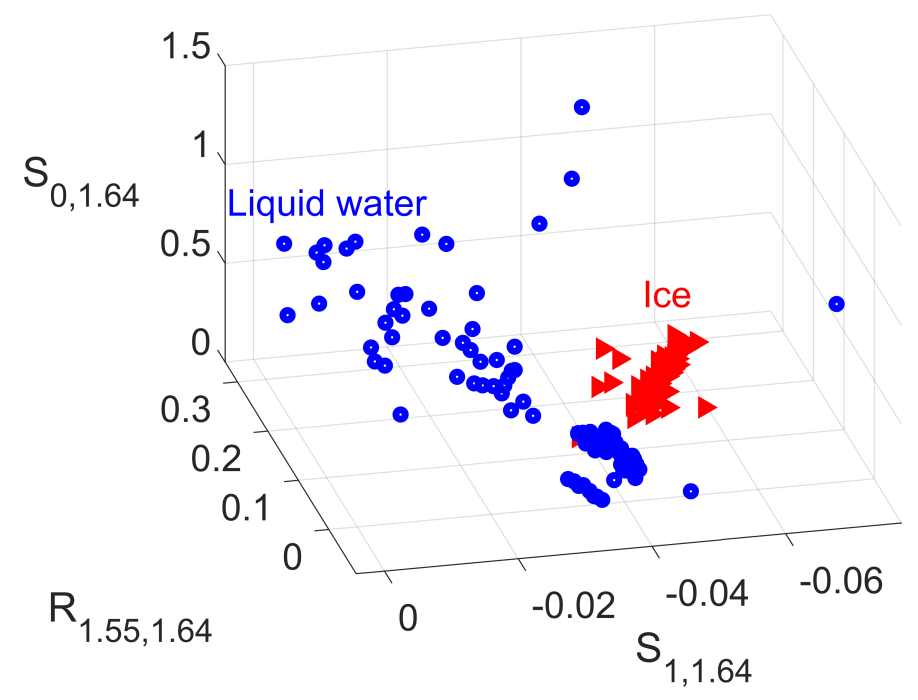


Figure 7. The combined method used an  $S_1$  parameter and had the best classification, suggesting that the addition of polarization sensitivity was helpful.

aerosol radiometers. In that capacity, meteorologists and climatologists would have another tool in their arsenal to better understand, model, and predict weather and climate. As a means to achieve that goal, this theory must be further vetted with more experimental data under a large amount of conditions to determine the true potential of the combined method.

#### ACKNOWLEDGMENTS

This work was funded by NASA EPSCoR grant NNX14AN40A and by the Air Force Office of Scientific Research under agreement number FA9550-14-1-0140. The U.S. Government is authorized to reproduce and distribute reprints for Governmental purposes notwithstanding any copyright notation thereon. The views and conclusions contained herein are those of the authors and should not be interpreted as necessarily representing the official policies or endorsements, either expressed or implied, of the Air Force Research Laboratory or the U.S. Government.

### REFERENCES

- Ramanathan, V., Cess, R. D., Harrison, E. F., Minnis, P., Barkstrom, B. R., Ahmad, E., and Hartmann, D., "Cloud-Radiative Forcing and Climate: Results from the Earth Radiation Budget Experiment," Science 243(4887), 57–63 (1989).
- [2] Boucher, O., Randall, D., Artaxo, P., Bretherton, C., Feingold, G., Forster, P., Kerminen, V.-M., Kondo, Y., Liao, H., Lohmann, U., Rasch, P., Satheesh, S., Sherwood, S., Stevens, B., and Zang, X.-Y., "2013: Clouds and Aerosols," tech. rep., Cambridge University Press, Cambridge, United Kingdom and New York, NY, USA (2013).
- [3] Rossow, W. B. and Schiffer, R. A., "Advances in Understandig Clouds from ISCCP," Bulletin of the American Meteorological Society 80(11), 2261–2288 (1999).
- [4] Wsicombe, W. J., "An absorbing mystery," Nature 376, 466–467 (1995).

- [5] Ramanathan, V., Subasilar, B., Zhang, G. J., Conant, W., Cess, R. D., Kiehl, J. T., Grassl, H., and Shi, L., "Warm Pool Heat Budget and Shortwave Cloud Forcing: A Missing Physics?," Science 267(5197), 499–503 (1995).
- [6] Key, J. R. and Intrieri, J. M., "Cloud Particle Phase Determination with the AVHRR," Journal of Applied Meteorology 39, 1797–1804 (oct 2000).
- [7] Flato, G., Marotzke, J., Abiodun, B., Braconnot, P., Chou, S. C., Collins, W., Cox, P., Driouech, F., Emori, S., Eyring, V., Forest, C., Gleckler, P., Guilyardi, E., Jakob, C., Kattsov, V., Reason, C., and Rummukainen, M., "2013: Evaluation of Climate Models," tech. rep., Intergovernmental Panel on Climate Change, Cambridge, United Kingdom and New York, NY, USA (2013).
- [8] Knap, W. H., Stammes, P., and Koelemeijer, R. B. A., "Cloud Thermodynamic-Phase Determination From Near-Infrared Spectra of Reflected Sunlight," *Journal of the Atmospheric Sciences* **59**, 83–96 (jan 2002).
- [9] Seldomridge, N. L., Shaw, J. A., and Repasky, K. S., "Dual-polarization lidar using a liquid crystal variable retarder," *Optical Engineering* **45**(10), 106202(1–10) (2006).
- [10] Martins, J. V., Marshak, A., Remer, L. A., Rosenfeld, D., Kaufman, Y. J., Fernandez-Borda, R., Koren, I., Correia, A. L., Zubko, V., and Artaxo, P., "Remote sensing the vertical profile of cloud droplet effective radius, thermodynamic phase, and temperature," *Atmospheric Chemistry and Physics* 11(18), 9485–9501 (2011).
- [11] King, M. D., Tsay, S.-C., Platnick, S. E., Wang, M., and Liou, K.-N., "Cloud Retrieval Algorithms for MODIS: Optical Thickness, Effective Particle Radius, and Thermodynamic Phase," Tech. Rep. 5, NASA Goddard Space Flight Center (dec 1997).
- [12] Thompson, D. R., McCubbin, I., Gao, B. C., Green, R. O., Matthews, A. A., Mei, F., Meyer, K. G., Platnick, S., Schmid, B., Tomlinson, J., and Wilcox, E., "Measuring cloud thermodynamic phase with shortwave infrared imaging spectroscopy," *Journal of Geophysical Research: Atmospheres* 121(15), 9174– 9190 (2016).
- [13] Jäkel, E., Walter, J., and Wendisch, M., "Thermodynamic phase retrieval of convective clouds: impact of sensor viewing geometry and vertical distribution of cloud properties," *Atmospheric Measurement Techniques* **6**(3), 539–547 (2013).
- [14] Hu, Y.-X., Winker, D., Yang, P., Baum, B., Poole, L., and Vann, L., "Identification of cloud phase from PICASSO-CENA lidar depolarization: a multiple scattering sensitivity study," *Journal of Quantitative Spectroscopy and Radiative Transfer* **70**(4-6), 569–579 (2001).
- [15] Tauc, M. J., Baumbauer, C. L., Moon, B., Eshelman, L. M., Nakagawa, W., Shaw, J. A., Abel, A. M., and Riesland, D. W., "Cloud thermodynamic phase detection with a 3-channel shortwave infrared polarimeter," in [Polarization: Measurement, Analysis, and Remote Sensing XIII], Chenault, D. B. and Goldstein, D. H., eds., SPIE 10655, 106550O, SPIE, Orlando, FL (may 2018).
- [16] Tauc, M. J., COMBINING SPECTRAL AND POLARIMETRIC METHODS TO CLASSFIY CLOUD THERMODYNAMIC PHASE, doctor of philosophy, Montana State University (2019).
- [17] Tauc, M. J., Nakagawa, W., and Shaw, J. A., "Influence of second-order reflections during polarimetric calibration with two wire-grid polarizers," *Optical Engineering* 58, 1 (mar 2019).
- [18] Sassen, K., "The Polarization Lidar Technique for Cloud Research: A Review and Current Assessment," Bulletin of the American Meteorological Society 72(12), 1848–1866 (1991).
- [19] Schotland, R. M., Sassen, K., and Stone, R., "Observations by Lidar of Linear Depolarization Ratios for Hydrometeors," *Journal of Applied Meteorology* **10**(5), 1011–1017 (1971).
- [20] Riedi, J., Doutriaux-Boucher, M., Goloub, P., and Couvert, P., "Global distribution of cloud top phase from POLDER/ADEOS I," *Geophysical Research Letters* **27**(12), 1707–1710 (2000).
- [21] Winker, D. M., Pelon, J., Coakley, J. A., Ackerman, S. A., Charlson, R. J., Colarco, P. R., Flamant, P., Fu, Q., Hoff, R. M., Kittaka, C., Kubar, T. L., Le Treut, H., McCormick, M. P., Mégie, G., Poole, L., Powell, K., Trepte, K., Vaughan, M. A., and Wielicki, B. A., "The Calipso Mission: A Global 3D View of Aerosols and Clouds," Bulletin of the American Meteorological Society 91(9), 1211–1229 (2010).
- [22] Shaw, J. A. and Pust, N. J., "Icy wave-cloud lunar corona and cirrus iridescence," Applied Optics **50**(28), F6–11 (2011).

- [23] Knobelspiesse, K., van Diedenhoven, B., Marshak, A., Dunagan, S., Holben, B., and Slutsker, I., "Cloud thermodynamic phase detection with polarimetrically sensitive passive sky radiometers," *Atmospheric Measurement Techniques* 8, 1537–1554 (mar 2015).
- [24] Holben, B., Eck, T., Slutsker, I., Tanré, D., Buis, J., Setzer, A., Vermote, E., Reagan, J., Kaufman, Y. J., Nakajima, T., Lavenu, F., Jankowiak, I., and Smirnov, A., "AERONETA Federated Instrument Network and Data Archive for Aerosol Characterization," *Remote Sensing of Environment* 66(1), 1–16 (1998).